This article has been accepted for publication in a future issue of this journal, but has not been fully edited. Content may change prior to final publication. Citation information: DOI 10.1109/ACCESS.2019.2941212, IEEE Access

IEEE Access
Multidisciplinary | Rapid Review | Open Access Journal

Compact Liquid Crystal Polymer Based Tri-Band Flexible Antenna for WLAN/WiMAX/5G Applications

CHENGZHU DU[1], XIAODI LI[1], and SHUNSHI ZHONG[2], (Member, IEEE)

[1]College of Electronics and Information Engineering, Shanghai University of Electric Power, Shanghai 200090, China

[2]School of Communication and Information Engineering, Shanghai University, Shanghai 200072, China

Corresponding author: CHENGZHU DU (e-mail: duchengzhu@163.com).

This work was supported by the National Science Foundation of China under Grant No. 61371022.

ABSTRACT In this paper, a new compact coplanar waveguide (CPW)-fed liquid crystal polymer (LCP) based tri-band antenna is presented and fabricated for Wireless Local Area Network (WLAN), Worldwide Interoperability for Microwave Access (WiMAX) and 5th-Generation (5G) systems. The antenna combines two strips with the main radiation rectangular patch and coplanar waveguide ground. The proposed antenna is printed on a LCP substrate with a thickness of 0.1 mm and has a small overall dimensions of 20mm×32mm×0.1mm. To analyze the characteristics, the antenna is designed and fabricated, and then the performance of the antenna is measured and tested. The measurement results show that the proposed antenna has three operating bandwidths, including 2.38-2.79 GHz, 3.27-4.05 GHz, and 4.80-8.44 GHz. To test the flexibility of the antenna, the antenna is simulated and measured in bent configurations for radii of 10 mm and 50 mm. In addition, the antenna is attached to different parts of the human body to test the integration effect in wearable equipment. The experimental results show that the performance of the antenna remains reliable under bending conditions and that the specific absorption ratio (SAR) value meets the European Union (EU) standard. The proposed antenna shows reasonable gains and good radiation characteristics in the operating bands. The flexible, compact, simple design and multiband performance indicates that the antenna is suitable for integration in flexible electronic devices.

INDEX TERMS LCP, WLAN/WiMAX/5G, Flexible antennas, CPW

I. INTRODUCTION

Wireless communication systems have been developing rapidly in recent years, and planar printed antennas have attracted extensive attention in academic and industrial circles due to their small size, light weight, simple processing, and easy integration [1]. A recent study on planar antennas focused on two research areas of interest: ultra-wideband and multi-frequency antennas [2]. Multi-frequency antennas for wireless systems used in Wireless Local Area Network (WLAN) and Worldwide Interoperability for Microwave Access (WiMAX) are an important application in these research areas. In addition, the China 5th-Generation (5G) spectrum resource allocation plan which requires the antenna to operate at: 3.4-3.5, 3.5-3.6, and 4.8-4.9 GHz announced by the Industrial Information Department of China at the end of 2018 places higher requirements on multi-frequency antenna.

Over the past few years, several designs have been investigated on multiband antennas for WLAN and WiMAX applications. L-shaped arms, a slitted feedline, and a slitted ground plane were used to excite three different resonances in [3]. The antenna in [4] was composed of a rectangular ring, a fork-shaped strip, a modified 1-shaped stub, and a coplanar waveguide to achieve tri-band operation. The antenna in [5] consisted of a small inner rectangular ring, an outer rectangular loop with three slits and a parasitic strip is exploited for WLAN and WiMAX application. The tri-band antenna in [6] was composed of a circle patch with a Complementary Split RingResonator (CSRR) slot and a conventional ground plane. By combining two ring-shaped strips with a new rectangular strip, tri-band antenna is proposed in [7]. A circular ring, a Y-shape-like strip, and a defected ground plane were used to design a triple-band antenna in [8]. The antenna in [9] was composed of a rectangular shaped radiator with F-shaped slots with the same geometry on the left and right sides. The comparison between the above antennas and the proposed antenna is shown in Table 1. The above antennas realize a dual or multi-frequency through different structures, but compared with the proposed antenna, the structure is complex, and the overall size of the antenna is larger. In addition, with the miniaturization and integration of various electronic devices, the ability of the antenna to bend in electronic equipment has become particularly important. Although the above antennas achieve a good multi-frequency function, they are printed on rigid FR4 substrate, which means that those antennas lack bending ability. In addition, the above antennas do not fully contain the China 5G spectrum.

In recent years, the application of conformal antenna and wearable antennas has been increasing, and research on flexible antennas has become popular [10-15]. Liquid crystal polymer (LCP) dielectric substrate is a flexible substrate material that has the advantages of low dielectric loss, low thermal expansion coefficient, and lower production cost. It has a stable dielectric constant over a wide frequency range, and is easy to fabricate into RF-integrated devices, which is suitable for printed antennas. An antenna array based on LCP substrate was presented in [16] but without flexibility analysis. A triple band-notched LCP-based Ultra Wide Band (UWB) monopole antenna in [17] was presented for flexible electronics; however, the antenna cannot operate at WLAN 2.4 GHz and there is little bending analysis available. A series-fed two-dipole antenna fabricated on a flexible LCP substrate using inkjet printing technology was presented in [18]. The bending behavior of the antenna is suitable, but it operates in a higher frequency band and cannot meet the bandwidth requirements of WLAN and WiMAX. Terahertz micro strip patch antenna arrays designed on LCP substrate is shown in [19]. The antenna is mainly used for cancer detection and vital sign detection on-body techniques. A wearable monopole antenna for the Wireless Body Area Network (WBAN) system based on LCP dielectric substrate was presented in [20]. The above LCP-based antennas are mainly designed as antenna arrays, band-notched antennas and dual-band antennas.

In this paper, a new compact coplanar waveguide (CPW)-fed LCP based tri-band antenna is presented for WLAN, WiMAX and 5G applications. The overall size of the antenna is 20mm×32mm×0.1mm, and the antenna is printed on a 0.1 mm LCP substrate, which means that the antenna is smaller than the traditional rigid antenna and can work in the bending state. It is fed by a CPW for good impedance matching and larger working bandwidth. In addition, both the radiation patch and the ground plane are designed on the same side of the LCP substrate, which helps to improve the antenna integration and reduce the manufacturing cost. By adding additional L-shaped strips to the main radiation patch and the coplanar waveguide ground, an effective triple band for WLAN, WiMAX, and 5G systems is obtained. The measured results are in good agreement with the simulation. The antenna design, parameter analysis, and experimental results such as S_{11}, radiation patterns and peak gain are discussed and given. In addition, the proposed antenna is tested and discussed in different bending circumstances. Furthermore, the antenna performance is measured on different positions on the body, and specific absorption ratio (SAR) performance is simulated on human body model by High Frequency Structure Simulator (HFSS).

TABLE 1. Antenna comparison.

Ref.	substrate	Size (mm ×mm)	Operating bands (GHz)
[3]	FR4	25 × 35	2.05–2.26, 3.41–3.82, 4.89–9.11
[4]	FR4	40 ×30	2.24–2.71, 3.4–4.5, 5.2-6.43
[5]	FR4	50 ×50	2.37-2.38, 5.15-5.85
[6]	FR4	35 ×35	2.4-2.48, 3.3-3.9, 5.15-5.7
[7]	FR4	35 ×26.6	3.19-4.57, 5.37-5.6, 7.56-10.67
[8]	FR4	25 ×38	2.39–2.6, 3.2–4.2, 5.09–5.82
[9]	FR4	27.5×26.6	0.85–0.95, 1.65–2.1, 2.4–3
Proposed	LCP	20 ×32	2.38-2.79, 3.27-4.05, 4.80-8.44

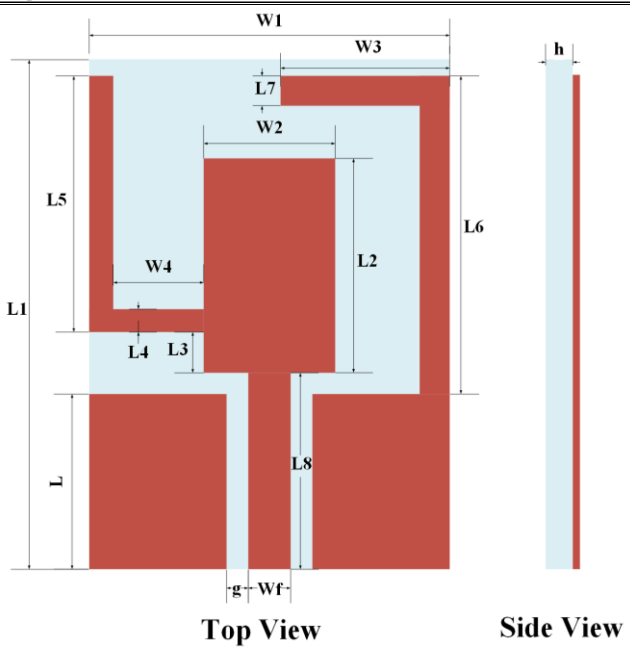

FIGURE 1. Geometry and dimensions of the proposed antenna.

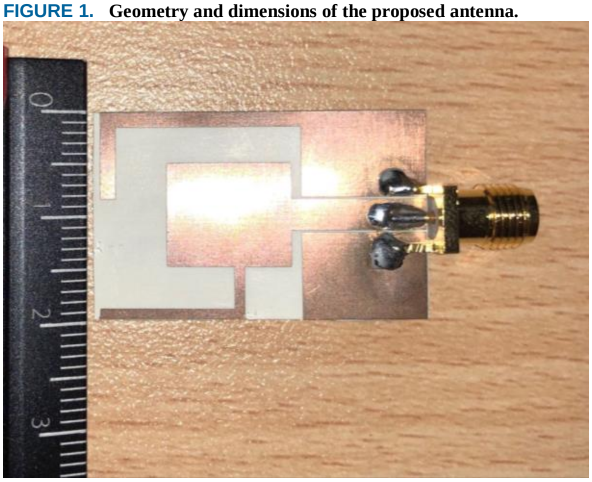

FIGURE 2. Photograph of the fabricated antenna.

This article has been accepted for publication in a future issue of this journal, but has not been fully edited. Content may change prior to final publication. Citation information: DOI 10.1109/ACCESS.2019.2941212, IEEE Access

II. ANTENNA DESIGN AND ANALYSIS

The configuration of the proposed tri-band antenna is presented in Fig. 1. The antenna is fabricated on an LCP substrate with a thickness of 0.1 mm, a relative permittivity (ε_γ) =2.9 and loss tangent ($\tan\delta$) =0.002. The overall dimensions ($W_1 \times L_1$) are 20mm×32mm. The proposed antenna is fed by CPW with a transmission width (W_f) of 3 mm, and the gap (g) on both sides of the transmission line is 0.2mm. The tri-band antenna is obtained by integrating two L-shaped strips, which are connected to the rectangular patch and the CPW ground patch, respectively. The dimensions of the antenna simulated and optimized by ANSYS HFSS are shown in Table 2. Fig. 2 shows the fabricated prototype of the antenna.

TABLE 2. Parameters of the proposed antenna.

Parameter	Value	Parameter	Value
L	12 mm	L_7	1.5 mm
L_1	32 mm	L_8	13 mm
L_2	12 mm	W_1	20 mm
L_3	4.5 mm	W_2	10 mm
L_4	1 mm	W_3	8.5 mm
L_5	14 mm	W_4	4 mm
L_6	19.5 mm	W_f	3 mm
h	0.1 mm	g	0.2 mm

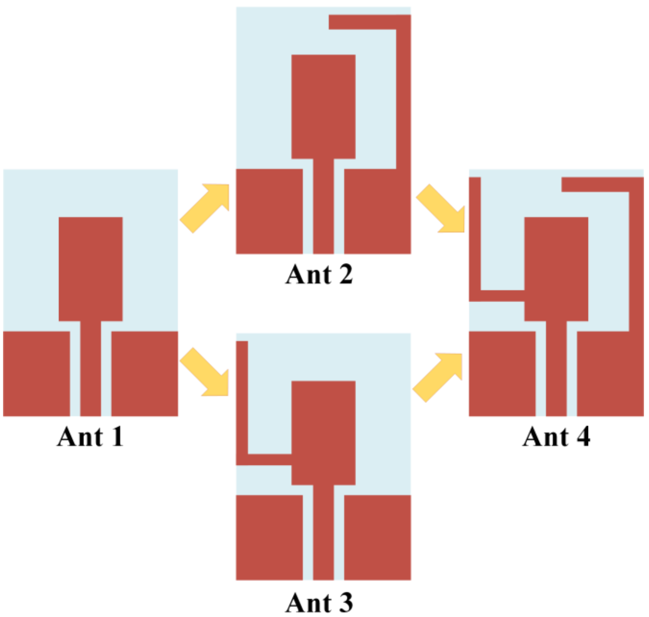

FIGURE 3. Antenna design evolution.

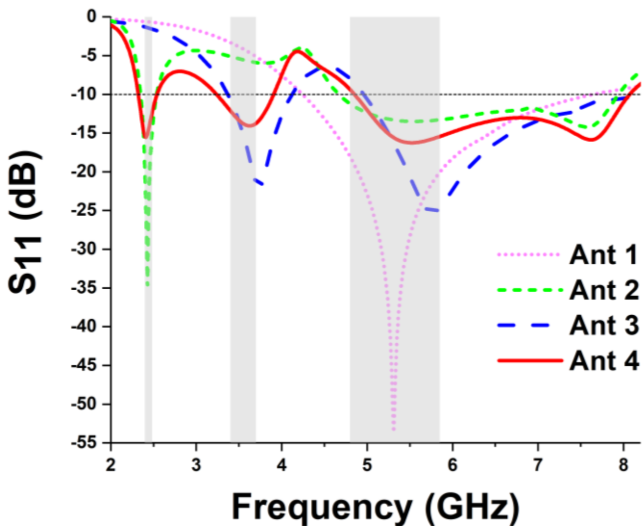

FIGURE 4. Simulated S_{11} of the various antennas involved.

Fig. 3 depicts the design process. The S_{11} curve of each antenna is shown in Fig. 4. The length and width of the rectangular patch are determined by the basic rectangular antenna equations [21, 22]. The length of each inverted-L strip (L_r) is found to be nearly a quarter of the dielectric wavelength calculated at the desired resonant frequency and can be calculated as:

$$L_r = \frac{C}{2f\sqrt{\varepsilon_{eff}}} \quad (1)$$

$$\varepsilon_{eff} \approx \frac{(\varepsilon_r + 1)}{2} \quad (2)$$

where C is the speed of light, f is the desired resonant frequency, and ε_{eff} is the effective relative permittivity.

The antenna design starts with a simple rectangular monopole antenna (see Ant1) with a CPW-fed that can obtain a large frequency bandwidth from 4.24-7.65 GHz, which covers the 4.9-GHz 5G, 5.5-GHz WiMAX and 5.2/5.8-GHz WLAN standard. Then, by attaching L-shaped strips, L_{r1} (L_6+W_3) and L_{r2} (L_5+W_4), on the ground of the CPW (see Ant 2) and the rectangular patch (see Ant 3) respectively, two resonant modes that cover 2.4-GHz WLAN and 3.5-GHz 5G/WiMAX were excited. Finally, Ant 1, Ant 2, and Ant 3 are combined into Antenna 4. The simulation results show that Antenna 4 realizes tri-band operation, and generates two resonance points near 2.4 GHz and 3.5 GHz. In addition, Antenna 4 retains the wide frequency band produced by the original rectangular monopole antenna.

The resonant characteristics of the antenna can be analyzed by the surface current distribution of the antenna. Fig. 5 shows the simulated current distribution of the antenna at frequencies of 2.4, 3.5 and 5.5 GHz. In Fig. 5(a), it can be observed that the current is mainly distributed in the left L-shaped strip. The current in Fig. 5(b) is mainly distributed in the right L-shaped strip. The result shows that the left and right L-shaped strips have the most significant effect on the generation of two resonance modes in the lower band and

This article has been accepted for publication in a future issue of this journal, but has not been fully edited. Content may change prior to final publication. Citation information: DOI 10.1109/ACCESS.2019.2941212, IEEE Access

middle band, respectively. As shown in Fig. 5(c), the currents are distributed at the left and right edges of the rectangular patch, especially on the two strips, which means that those parts affect the upper band. The current of the CPW transmission line at different frequency points is large in Fig. 5, indicating that the antenna is in operation and has good impedance matching. According to the current distribution of the above three frequencies, the parameter simulation analysis, which is given in Fig. 6-8, is carried out on the length of both strips (L_5, W_3) and the length of the rectangular patch (L_2).

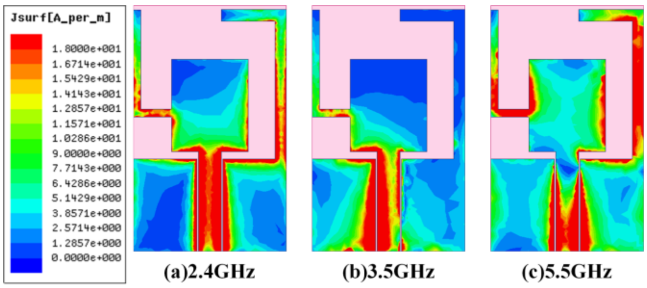

FIGURE 5. Simulated current distributions of the proposed antenna at (a) 2.4, (b) 3.5, and (c) 5.5 GHz.

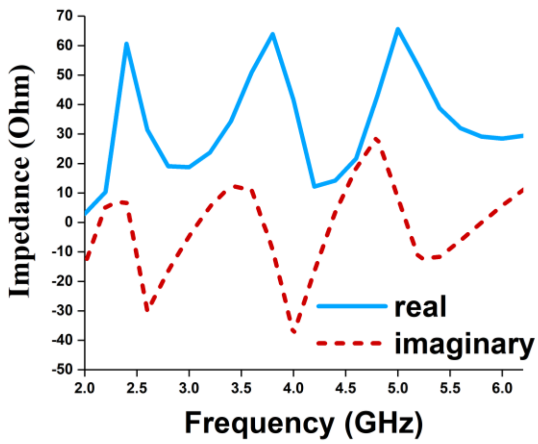

FIGURE 6. Input impedance curves of the proposed antenna.

The impedance characteristics of the above antenna are shown in Fig. 6, and it can be clearly seen that there is good impedance matching in the operating band.

The length of the rectangular patch (L_2) has a great influence on the upper bandwidth. Figure 7 shows that as the length of the rectangular patch increases, the bandwidth shifts left and the bandwidth becomes wider, whereas the other two bands did not change significantly. In Fig. 8 and Fig. 9, the effect of the strip length (L_5 and W_3) on the antenna's performance is studied. The results show that the increase of L_5 not only achieves good impedance matching in the middle band but also enlarges the middle bandwidth of the proposed antenna. The increase of W_3 causes lower band shifts to lower frequencies. Thus, by adjusting the length of L_5 and W_3, the middle and lower bands can be changed. In addition, the change of length only affects the corresponding bandwidth but does not affect other bands. In summary, the above results are completely consistent with the results of the antenna surface distribution, which indicates that the antenna is easy to design and adjust.

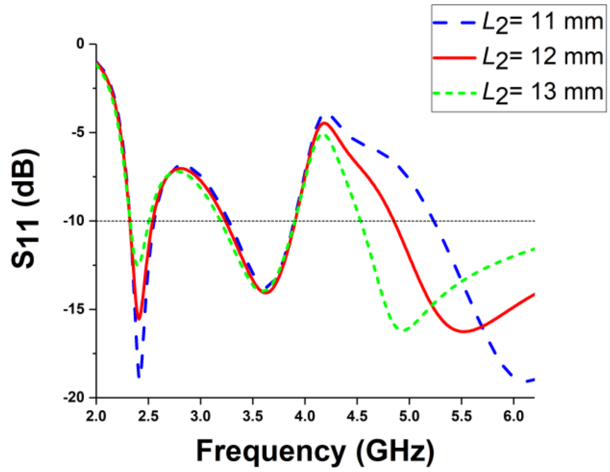

FIGURE 7. Simulated S_{11} with different lengths of L_2.

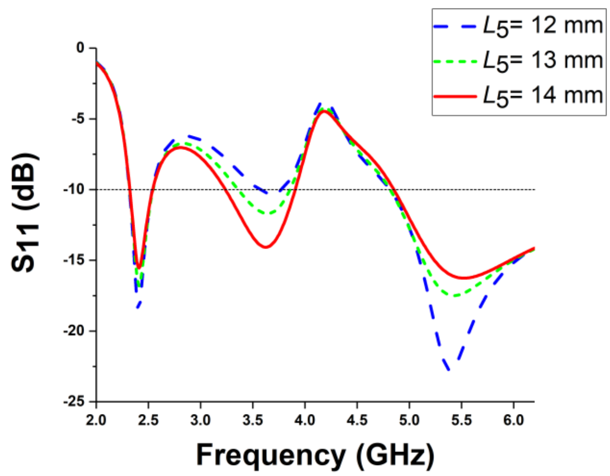

FIGURE 8. Simulated S_{11} with different lengths of L_5.

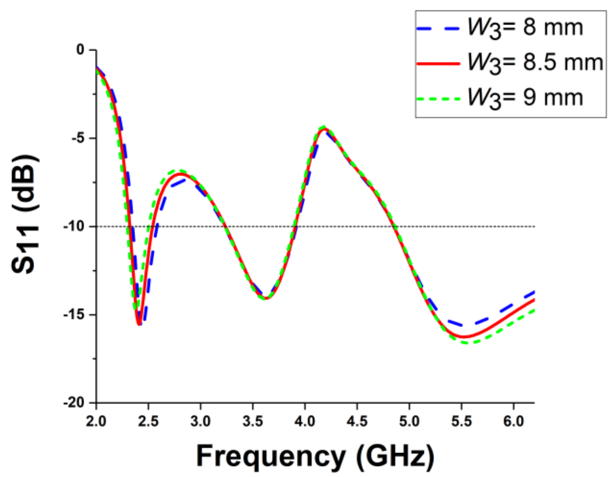

FIGURE 9. Simulated S_{11} with different lengths of W_3.

This article has been accepted for publication in a future issue of this journal, but has not been fully edited. Content may change prior to final publication. Citation information: DOI 10.1109/ACCESS.2019.2941212, IEEE Access

III. ANTENNA PERFORMANCES

A. MEASUREMENTS RESULTS

Based on the above conclusions, the antenna prototype was fabricated and measured. The simulated and measured S_{11} are depicted in Fig. 10. The measured and simulated results are in good agreement; the three operating bands of the measured results have a wider bandwidth than the simulation results, and the antenna has good impedance matching at 2.5, 3.5, and 5.5 GHz. The measured bandwidths with a -10 dB return loss are approximately 410 MHz (2.38-2.79 GHz), 780 MHz (3.27-4.05 GHz), 3640 MHz (4.80-8.44 GHz), which successfully fulfills the operating bands for the WLAN, WiMAX and 5G systems.

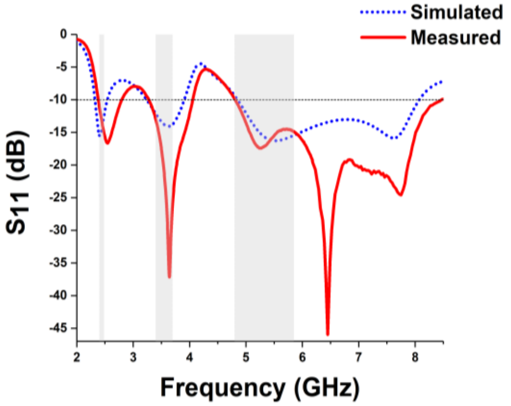

FIGURE 10. **Measured and simulated results for S_{11}.**

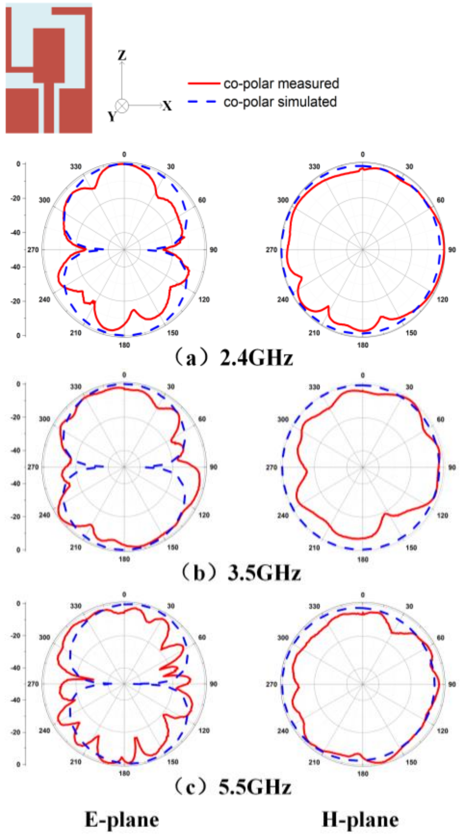

FIGURE 11. **Measured and simulated radiation patterns of the proposed antenna at (a) 2.4, (b) 3.5, and (c) 5.5GHz.**

The simulated and measured far-field radiation patterns at frequencies of 2.4, 3.5, and 5.5 GHz are depicted in Fig. 11. It can be concluded that the H-plane (*xy*-plane) of the antenna has almost omnidirectional radiation and that the E-plane (*yz*-plane) is bidirectionally radiated. TABLE 3 and Fig. 12 show the simulated and measured peak gains at the desired bands. The obtained average gains are approximately 0.65, 2.26, and 2.61 dBi for the 2.4, 3.5, and 5.5 GHz bands, respectively.

TABLE 3. **Simulated and measured gain.**

Frequency (GHz)	Measured Gain (dBi)	Simulated Gain (dBi)
2.4	0.65	0.31
3.5	2.26	2.28
5.5	2.61	2.21

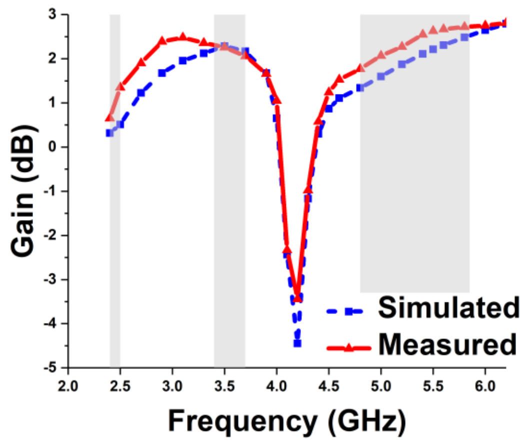

FIGURE 12. **Measured peak gain of the proposed antenna**

B. BENDING PERFORMANCE

The bent characteristic of the LCP dielectric substrate allows the antenna to be integrated into various electronic devices in a curved configuration, therefore, bending tests are important and necessary. To test the bending performance of the antenna, the bending models, including the E-plane and H-plane bending and the concave-convex bending, were simulated using HFSS software. In addition, the above two curve modes correspond to two bending radii (*R*=10 mm and *R*=50 mm), respectively.

The S_{11} in the above bending condition and the flat state are compared in Fig. 13. When *R* decreases, whether the E-plane or the H-plane is curved, the simulated S_{11} of the antenna decreases in all frequency bands.

When *R*=50 mm, the simulation results show that the antenna can maintain the tri-band operation when the H-plane is bent in this case. Meanwhile, the antenna changes from tri-band operation to dual-band operation when the E-plane bent at this radius. When *R*=10 mm, the antenna is a dual-frequency operation with H-plane bending, and the antenna becomes a single band under E-plane bending. Therefore, compared to E-plane bending, the antenna is more stable under H-plane bending. Moreover, compared with the flat state, the simulated results show that the resonance points

IEEE Access
Multidisciplinary : Rapid Review : Open Access Journal

of the three bands are shifted right of 50-500 MHz when the H-plane is rolled. It can be observed from Fig. 13 that the E-plane has a much smaller effect on the shifts of the resonance point compared with the H-plane. In addition, the proposed antenna can achieve good impedance matching under a concave configuration.

Fig. 14 and Fig. 15 depict the measured S_{11} of the bent antenna compared to the simulated one under different bending conditions. Moreover, the measured S_{11} of the bent antenna also contrasts with the flat antenna, and the analysis results are as follows. When the cylinder radius is 50mm, compared with the flat state, whether the E-plane or the H-plane is curved, it can be observed that a maximum shift of the antenna is 50-300 MHz in all frequency bands, and the S_{11} of the proposed antenna still satisfies less than -10 dB at the desired operating frequencies. In the case of high curvature bending (R=10 mm), the waveform of S_{11} varies greatly. When the H-plane was rolled on the cylinders, the S_{11} of the upper band clearly decreased. In addition, the middle and the lower band have a trend of connectivity. More changes occurred when the E-plane was rolled on the cylinder. The lower and middle bands of the antenna disappear and form a new bandwidth. At this time, the upper band of the antenna shifts left and the upper bandwidth increases. The antenna changes from tri-band operation to dual-band operation. In summary, the intended bandwidth of the antenna is conserved in both cases, and the performance of the antenna is still reliable under bending conditions.

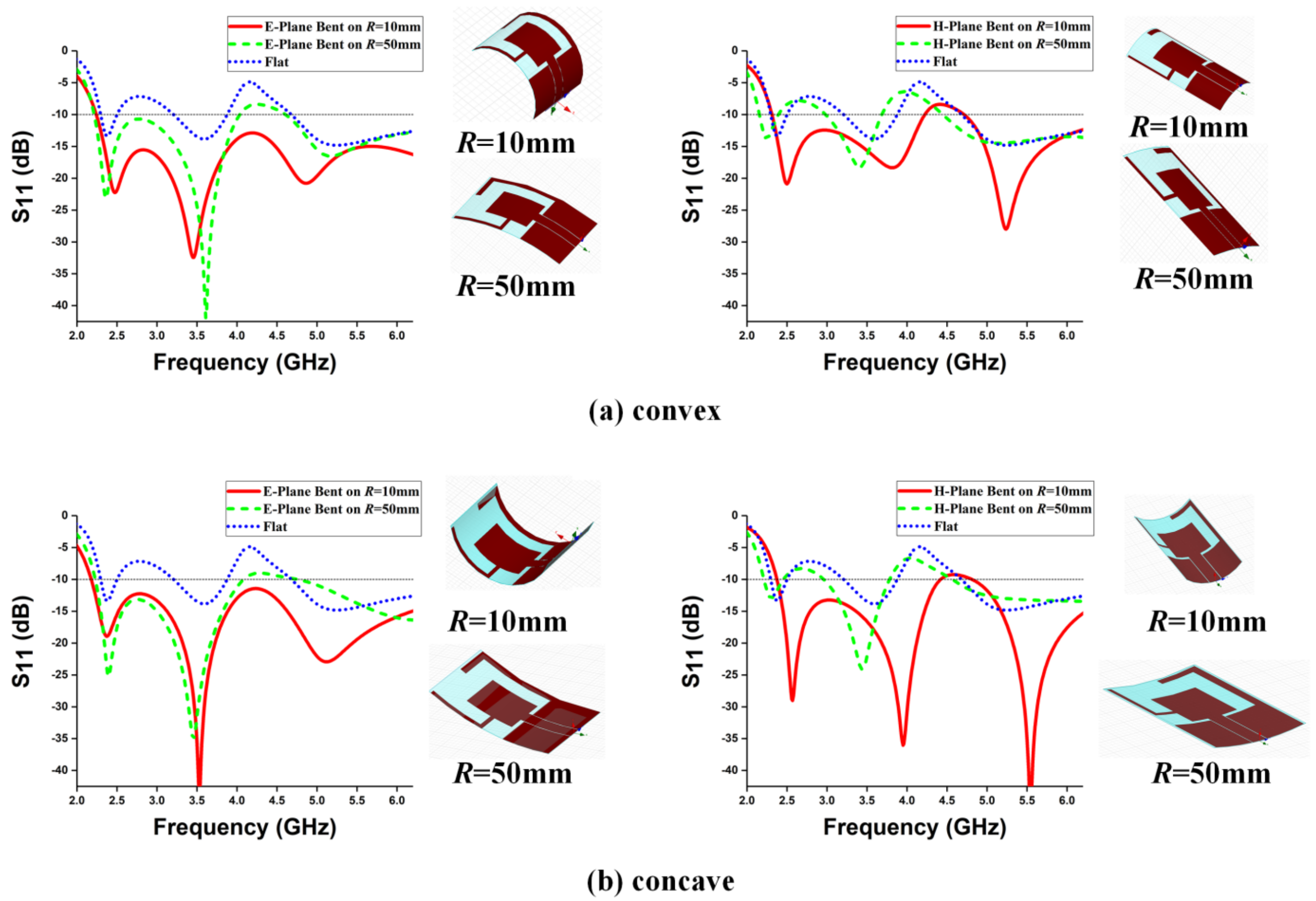

FIGURE 13. **Simulated E-plane and H-plane S_{11} for the proposed antenna rolled on a cylinder with two different radii in (a) convex and (b) concave configuration**

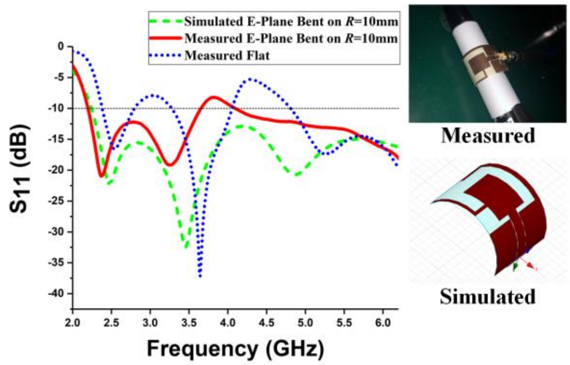

(a)

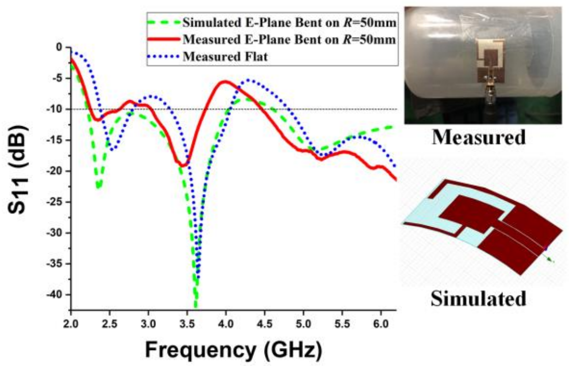

(b)

FIGURE 14 Measured and simulated S_{11} for the proposed antenna when E-lane rolled on a cylinder with two different radii (a) *R*=10 mm and (b) *R*=50 mm

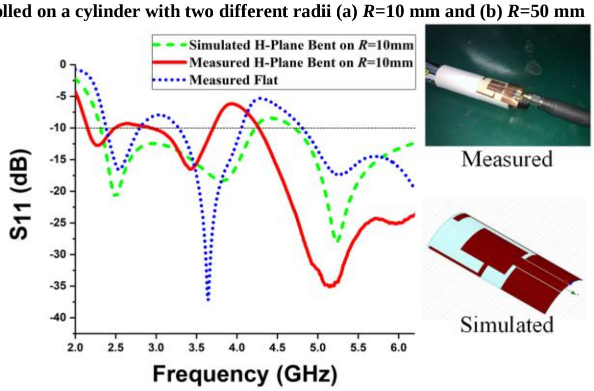

(a)

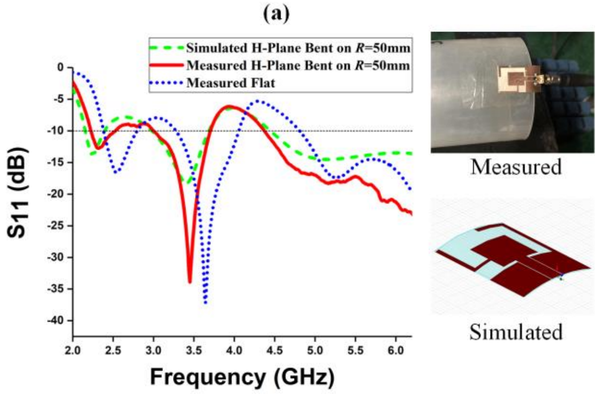

(b)

FIGURE 15. Measured and simulated S_{11} for the proposed antenna when H-plane rolled on a cylinder with two different radii (a) *R*=10 mm and (b) *R*=50 mm

Compared to traditional rigid dielectric substrates, LCP is ultrathin, has better dimensional stability and has better bending and stretching capabilities [23]. It is necessary to test the limit bending capability of the proposed antenna. The bending limit test and comparison are shown in Fig. 16. The E and H-planes of the antenna are wrapped to the limit condition and the bending radii are 5 mm and 3.5 mm, respectively. Although the S_{11} test shows that the return loss under limit bending varies greatly, in the operating frequency band, it is still less than -6 dB, which meets the actual engineering requirements.

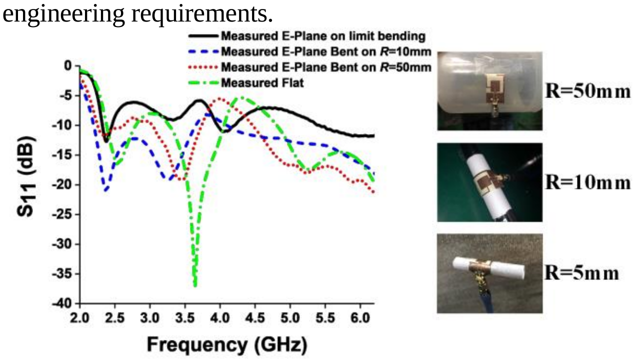

(a)

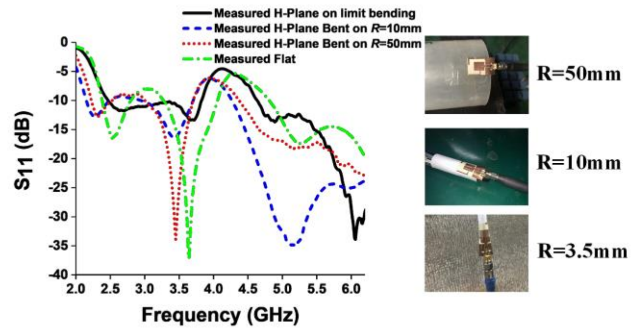

(b)

FIGURE 16. Comparison of the proposed antenna under limit bending conditions (a) E-plane and (b) H-plane

Fig. 17 and Fig. 18 show the radiation patterns in the bent configurations. The more the antenna bends, the more the radiation pattern changes. Although the antenna is curled, it still has omnidirectional radiation capability.

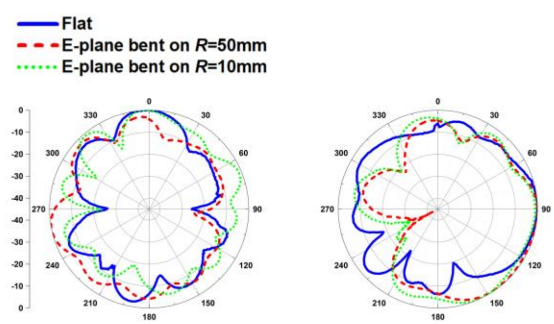

(a) 2.4GHz

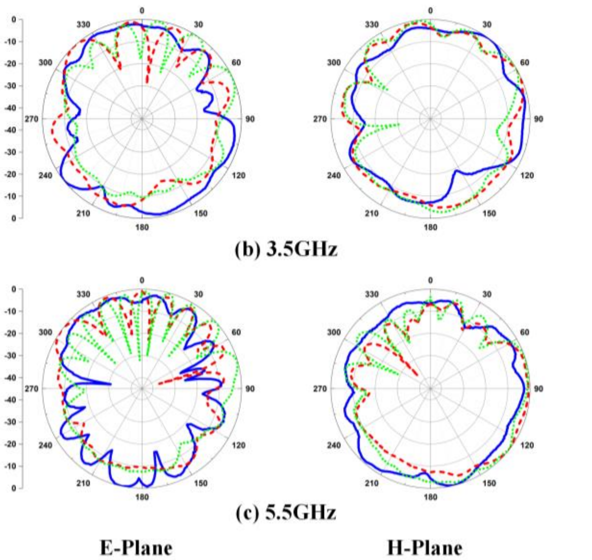

FIGURE 17. **Measured far-field radiation patterns at (a) 2.4, (b) 3.5, and (c) 5.5 GHz with E-plane under different bending conditions.**

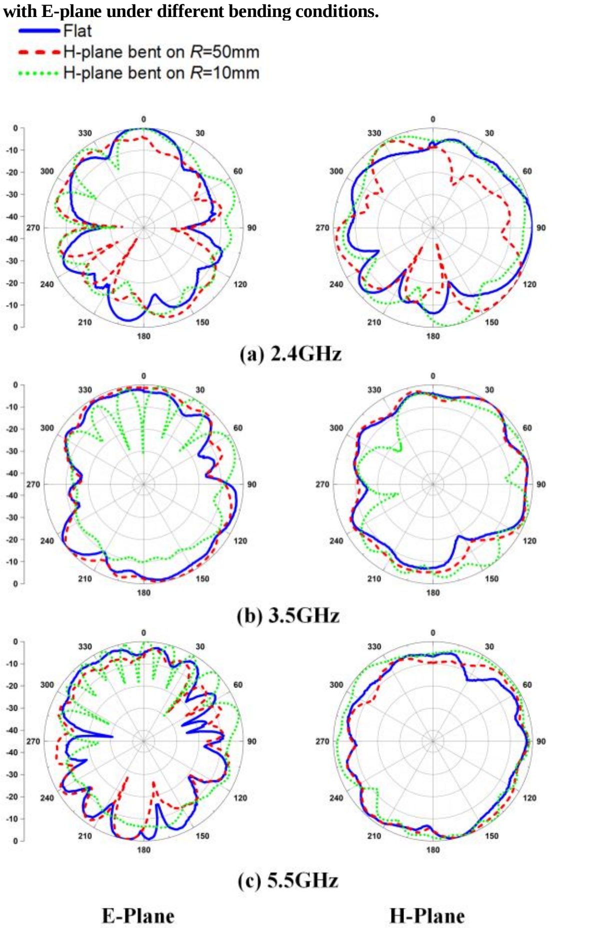

FIGURE 18. **Measured far-field radiation patterns at (a) 2.4, (b) 3.5, and (c) 5.5 GHz with H-plane under different bending conditions.**

C. ON-BODY PERFORMANCE

S_{11} was measured when the antenna was attached to different parts of the human body. The distance from the body to the proposed antenna is approximately 5 mm. The curvature of the antenna on the chest, leg, and wrist surface increases in turn. The results in Fig. 19 show that the operating band less than -10 dB as the standard, the antenna experiences tri-frequency, dual-frequency, and broadband operation as the curvature of the antenna becomes larger. This is in agreement with the results of previous bending analyses.

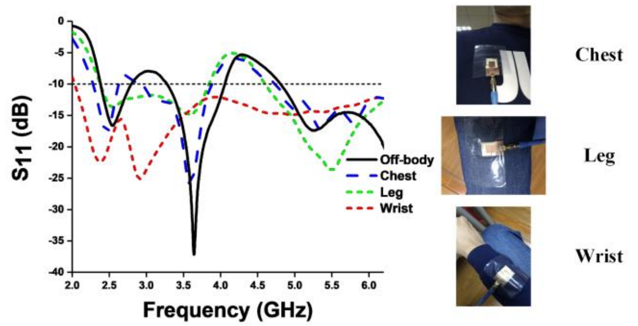

FIGURE 19. **Measured S_{11} of the suggested antenna on chest, leg, wrist, and off-body**

The SAR represents the electromagnetic radiation energy absorbed by a unit mass of material per unit time and can be calculated as:

$$SAR = \frac{\sigma E^2}{\rho} \tag{3}$$

where ρ is the mass density, E is the electric field intensity and σ is conductivity [24, 25].

The SAR for the antenna is calculated using HFSS. As shown in Fig. 20, the human tissue model contains a 2 mm skin layer, a 5 mm fat layer and a 20 mm muscle layer. The detailed parameters of each tissue are shown in Table 4 [26]. The overall size of the model is 42 mm× 30 mm× 27 mm. The distance between the antenna and the model is H_1.

TABLE 4. **Material properties of tissue.**

	Skin	Fat	Muscle
ε_r	37.95	5.27	52.67
σ (S/m)	1.49	0.11	1.77
Density (kg/m^3)	1001	900	1006
Thickness (mm)	2	5	20

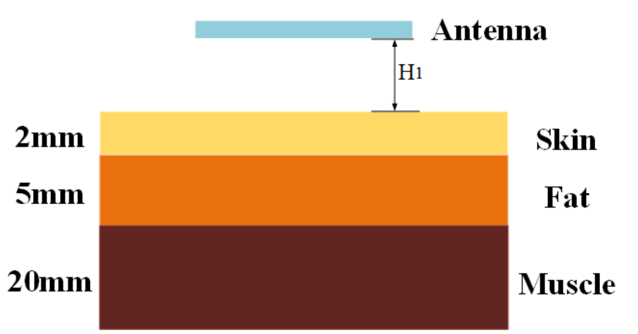

FIGURE 20. **Human tissue model**

Fig. 21 shows the SAR distribution when H_1 is 5 mm. The input power to the antenna is set to 0.2 W and the SAR results are shown in Table 5. The SAR distribution is shown in Fig. 21. The SAR level is below the European Union (EU) standard of 2 W / kg / 10 g tissue.

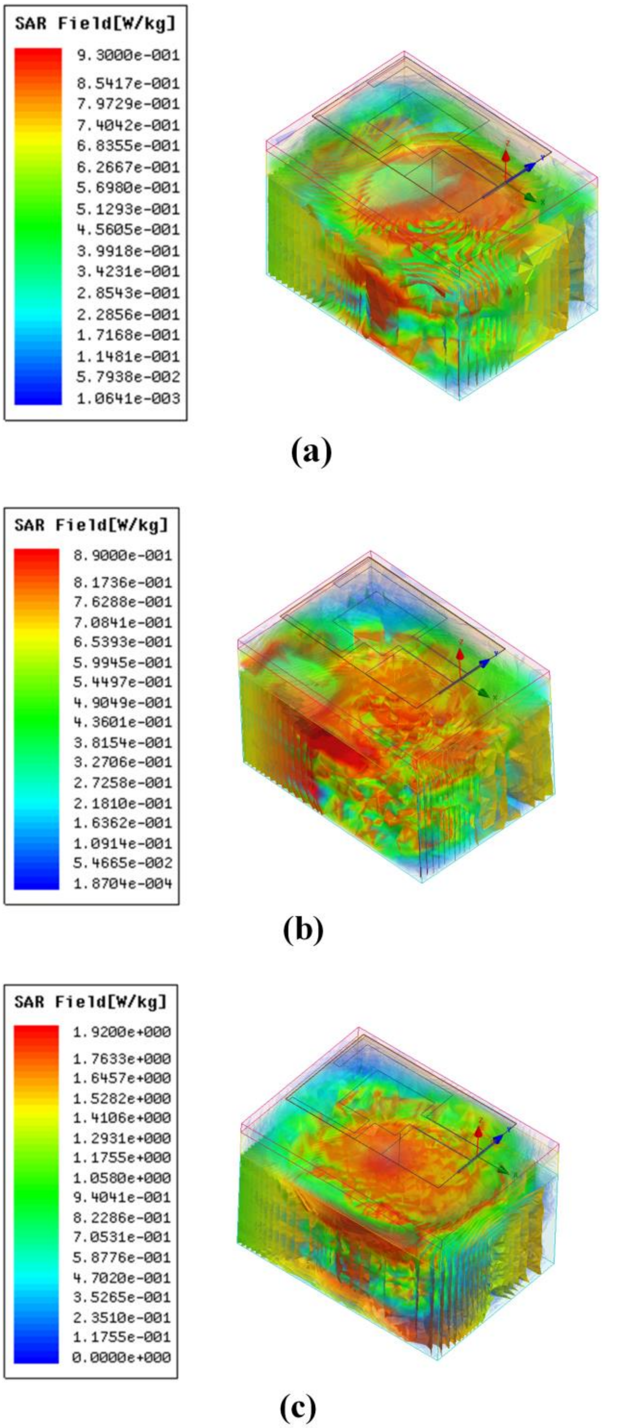

FIGURE 21. Simulated SAR distribution in 10 g tissues on the human tissue model (a) 2.4 GHz (b) 3.5 GHz (c) 5 GHz

TABLE 5. Maximum SAR values with different frequencies.

Frequency (GHz)	2.4	3.5	5
10 g Tissue (W/kg)	0.93	0.89	1.92

Ⅳ. CONCLUSION

In this paper, a compact CPW-fed LCP based tri-band antenna is presented. The antenna size is 20 mm×32 mm×0.1 mm. By adding additional radiation strips to the main radiation patch and the coplanar waveguide ground, the antenna can achieve three sufficient impedance bandwidths. The antenna prototype which has a compact and simple structure is fabricated and measured. The results show that the antenna has reasonable gain and good radiation characteristics. In addition, the proposed antenna is tested under different bending effects. The measured result shows that the antenna still retains the matching and good radiation patterns at the desired operating frequencies, in addition to the SAR meeting EU standards. A compact size, flexible substrate and simple structure are the advantages of the proposed antenna, which can be applied to WLAN, WiMAX and 5G devices.

REFERENCES

[1] L. Li, X. Zhang, X. Yin and L. Zhou, "A Compact Triple-Band Printed Monopole Antenna for WLAN/WiMAX Applications," in *IEEE Antennas and Wireless Propagation Letters*, vol. 15, pp. 1853-1855, 2016.
[2] M. Shuhrawardy, M. H. M. Chowdhury and R. Azim, "Design of a compact triple-band antenna for WLAN/WiMAX applications," *2017 3rd International Conference on Electrical Information and Communication Technology (EICT)*, Khulna, 2017, pp. 1-5.
[3] K. O. Gyasi *et al*., "Tri-band planar monopole antenna with two circularly polarised bandwidths for WiMAX applications," in *IET Microwaves, Antennas & Propagation*, vol. 12, no. 15, pp. 2350-2355, 19 12 2018.
[4] K. Yu and X. Liu, "Design of tri-band antenna with rectangular ring for WLAN and WiMAX application," *2017 Sixth Asia-Pacific Conference on Antennas and Propagation (APCAP)*, Xi'an, 2017, pp. 1-3.
[5] F. Liu, K. Xu, P. Zhao, L. Dong and G. Wang, "Uniplanar dual-band printed compound loop antenna for WLAN/WiMAX applications," in *Electronics Letters*, vol. 53, no. 16, pp. 1083-1084, 3 8 2017.
[6] K. Yu, Y. Li and Y. Wang, "Multi-band metamaterial-based microstrip antenna for WLAN and WiMAX applications," *2017 International Applied Computational Electromagnetics Society Symposium - Italy (ACES)*, Florence, 2017, pp. 1-2.
[7] M. N. Shakib, M. Moghavvemi and W. N. L. Binti Wan Mahadi, "Design of a Tri-Band Off-Body Antenna for WBAN Communication," in *IEEE Antennas and Wireless Propagation Letters*, vol. 16, pp. 210-213, 2017.
[8] P. Thawait and N. Kumar, "Triple band microstrip-fed antenna with defected ground plane for Bluetooth/WiMAX/WLAN," *2016 International Conference on Wireless Communications, Signal Processing and Networking (WiSPNET)*, Chennai, 2016, pp. 918-921.
[9] V. Sittakul, "Compact tri-band F-shaped slot antenna using complementary split ring resonator for mobile and WLAN applications," *2017 14th International Conference on Electrical Engineering/Electronics, Computer, Telecommunications and Information Technology (ECTI-CON)*, Phuket, 2017, pp. 431-434.
[10] A. Hachi, H. Lebbar and M. Himdi, "Flexible and conformal printed monopoles for reconfigurable antennas," *2017 11th European Conference on Antennas and Propagation (EUCAP)*, Paris, 2017, pp. 3057-3060.
[11] H. Kao *et al*., "Bending Effect of an Inkjet-Printed Series-Fed Two-Dipole Antenna on a Liquid Crystal Polymer Substrate," in *IEEE Antennas and Wireless Propagation Letters*, vol. 13, pp. 1172-1175, 2014.
[12] H. R. Khaleel, H. M. Al-Rizzo, D. G. Rucker and S. Mohan, "A Compact Polyimide-Based UWB Antenna for Flexible Electronics,"

in *IEEE Antennas and Wireless Propagation Letters*, vol. 11, pp. 564-567, 2012.

[13] S. Ahmed, F. A. Tahir, A. Shamim and H. M. Cheema, "A Compact Kapton-Based Inkjet-Printed Multiband Antenna for Flexible Wireless Devices," in *IEEE Antennas and Wireless Propagation Letters*, vol. 14, pp. 1802-1805, 2015.

[14] Yalavarthi, U. D, M. S. S, R, and B. T. P, M, "Liquid crystal polymer based flexible and conformal 5G antenna for vehicular communication," *in Materials Research Express*, vol. 6, pp. 1-12, 2019.

[15] Y. Usha Devi, M. S. S. Rukmini, and B. T. P. Madhav, "A Compact Conformal Printed Dipole Antenna for 5G Based Vehicular Communication Applications," *Progress In Electromagnetics Research C*, Vol. 85, 191-208, 2018.

[16] S. F. Jilani, M. O. Munoz, Q. H. Abbasi and A. Alomainy, "Millimeter-Wave Liquid Crystal Polymer Based Conformal Antenna Array for 5G Applications," in *IEEE Antennas and Wireless Propagation Letters*, vol. 18, no. 1, pp. 84-88, Jan. 2019.

[17] W. Xiao, T. Mei, Y. Lan, Y. Wu, R. Xu and Y. Xu, "Triple band-notched UWB monopole antenna on ultra-thin liquid crystal polymer based on ESCSRR," in *Electronics Letters*, vol. 53, no. 2, pp. 57-58, 19 1 2017.

[18] H. Kao *et al*., "Bending Effect of an Inkjet-Printed Series-Fed Two-Dipole Antenna on a Liquid Crystal Polymer Substrate," in *IEEE Antennas and Wireless Propagation Letters*, vol. 13, pp. 1172-1175, 2014.

[19] M. S. Rabbani and H. Ghafouri-Shiraz, "Liquid Crystalline Polymer Substrate-Based THz Microstrip Antenna Arrays for Medical Applications," in *IEEE Antennas and Wireless Propagation Letters*, vol. 16, pp. 1533-1536, 2017.

[20] S. R. Zahran, M. A. Abdalla and A. Gaafar, "New thin wide-band bracelet-like antenna with low SAR for on-arm WBAN applications," in *IET Microwaves, Antennas & Propagation*, vol. 13, no. 8, pp. 1219-1225, 3 7 2019.

[21] R. Garg, P. Bhartia, I.Bahl, A.Ittipiboon, “Microstrip Antenna Design Handbook”, Artech House inc.,2001.

[22] M. I. Hasan, M. A. Motin and M. S. Habib, "Circular ring slotting technique of making compact microstrip rectangular patch antenna for four band applications," *2013 International Conference on Informatics, Electronics and Vision (ICIEV)*, Dhaka, 2013, pp. 1-4.

[23] Lan, Y and Xu, Y, "Bending Limit Tests for Ultra-Thin Liquid Crystal Polymer Substrate Based on Flexible Microwave Components," in *Micromachines*, vol. 9, 2018.

[24] K. N. Paracha *et al*., "A Low Profile, Dual-band, Dual Polarized Antenna for Indoor/Outdoor Wearable Application," in *IEEE Access*, vol. 7, pp. 33277-33288, 2019.

[25] Y. J. Li, Z. Y. Lu and L. S. Yang, "CPW-Fed Slot Antenna for Medical Wearable Applications," in *IEEE Access*, vol. 7, pp. 42107-42112, 2019.

[26] G. Gao, B. Hu, S. Wang and C. Yang, "Wearable Circular Ring Slot Antenna With EBG Structure for Wireless Body Area Network," in *IEEE Antennas and Wireless Propagation Letters*, vol. 17, no. 3, pp. 434-437, March 2018.

CHENGZHU DU was born in Haikou, Hainan Province, China. She received the B.S. degree from the Xidian University, M.S. degree from Nanjing University of Posts and Telecommunications and PhD degree from Shanghai University, in 1995, 2003 and 2012, respectively, all in electromagnetic wave and microwave technology. She is currently an associate Professor of Shanghai University of Electric Power. Her research interests include flexible antenna and textile antenna, multiband and wideband antennas, and MIMO technologies.

XIAODI LI was born in Dezhou, Shandong Province, China in 1995. He received the B.S. degree from the Shandong Agricultural University in 2016. He is currently pursuing the M.S degree in College of Electronics and Information Engineering, Shanghai University of Electric Power. His research interests include multiband antenna, flexible antenna, and the antenna for partial discharge detection.

SHUNSHI Zhong (SM'94) was born in Zhejiang, China. He graduated from the Department of Radar Engineering, Xidian University (formerly Northwest Telecommunication Engineering Institute), Xi'an, China. He joined the faculty of the institute, and from 1970 to 1973, he worked on the development of a three-dimensional radar system at the Shanghai Factory of Test Equipment. From 1975 to 1979, he worked at the design of a radiotelescopy system for the Purple Mountain Observatory of Chinese Academy of Sciences, Nanjing, China. From 1980 to 1981, he was a Visiting Scholar at the University of Washington, Seattle, and from 1981 to 1982, the University of Illinois at Urbana-Champaign, later as a Research Consultant. From 1988 to 1994, he was with the Shanghai University of Science and Technology, where he was a professor and Director of Electromagnetic Laboratory. In 1993 he was elected as a supervisor of Ph.D. degree students in the Electromagnetic Fields and Microwave Techniques Study by the National Academic Degree Committee of China. Since 1994 he has been a professor at Shanghai University, China, and has graduated 20 Ph.D. degree students. He is the author of Microstrip Antenna Theory and Application (Xidian University Press, 1991), Foundation of Electromagnetic Field Theory (Xidian University Press, 1995), Fundamentals of Electromagnetic Fields (Tsinghua University Press, 2007), Antenna Theory and Techniques (Publishing House of Electronics Industry, 2011), a few book chapters, and is the co-translator of the Chinese edition of Antenna Theory: Analysis and Design (Publishing House of Electronics Industry, 1988). He also wrote five items (microstrip antenna, slot antenna, reflector antenna, etc.) for The Chinese Grand Encyclopedia-Electronics and Computers (1986). He holds eight patents. He has published over 200 journal papers and over 100 conference papers.

Prof. Zhong is a fellow of the Chinese Institute of Electronics (CIE) and served as Deputy Chairman of the Nanjing Joint Chapter, IEEE. He received a National Award in STA (Science and Technology Advancement), and a total of six Ministry/Province Awards in STA. He also received two Outstanding Textbook Awards. He is the recipient of the Governmental Special Allowance Award of China and the Bao-Gang Outstanding Teacher Award. He has served as a TPC member and session chair for a number of international conferences, and as a reviewer for the IEEE Transactions on Antennas and Propagation and other prestigious journals. He is on the editorial boards of the Chinese Journal of Radio Science and others. He has been listed in “Marquis Who is Who in the World” since 1996, and listed in “Outstanding People of the 20th Century” of IBC, Cambridge, U.K., 2001.